

# Effects of Base $\pi$ -Stacking on Damage to DNA by Low-Energy Electrons

Iwona Anusiewicz,<sup>†,‡,§</sup> Joanna Berdys,<sup>†,‡</sup> Monika Sobczyk,<sup>†,‡</sup> Piotr Skurski,<sup>†,‡</sup> and Jack Simons<sup>\*,†</sup>

Chemistry Department and Henry Eyring Center for Theoretical Chemistry, University of Utah, Salt Lake City, Utah 84112 and Department of Chemistry, University of Gdansk, 80-952 Gdansk, Poland

Received: June 16, 2004; In Final Form: July 28, 2004

In this work, we extend our earlier studies on single-strand break (SSB) formation in DNA to include the effects of base  $\pi$ -stacking. In these studies, we consider SSBs induced by low-energy electrons that attach to DNA bases'  $\pi^*$  orbitals. Here, we conclude that the inclusion of  $\pi$ -stacking effects causes an increase of the energy barriers (corresponding to accessing the stretched C–O bond that break in the SSB formation) that govern the rates of SSB formation. As a result, the rates of SSB formation are predicted (in the CCC codon considered here) to lie below  $0.8 \times 10^5 \text{ s}^{-1}$  for electrons having kinetic energies  $E \leq 2.0 \text{ eV}$  and thus to be not very competitive with electron autodetachment whose rate is ca.  $10^{14} \text{ s}^{-1}$ . However, in the presence of even modest solvation, autodetachment is rendered inoperative, so SSBs can occur with considerable yield via the electron-attachment pathway. In addition to these studies of sugar–phosphate C–O bond cleavage, we find that the barrier height for sugar–cytosine N–C bond breaking is 43 kcal/mol, which is much higher than the corresponding value estimated for the sugar–phosphate C–O bond breaking, which makes the N–C route not likely to be operative in such electron-induced SSBs.

## I. Introduction

There has been considerable recent interest<sup>1</sup> in the fact that low-energy electrons (i.e., electrons below ionization or electronic excitation thresholds) have been observed to damage DNA and in the mechanisms by which this can occur. This group's involvement in the study of how low-energy electrons may damage DNA was nurtured by beautiful experiments from Boudaiffa et al.<sup>2</sup> who observed single-strand breaks (SSBs) to occur in relatively dry samples of DNA<sup>3</sup> when free electrons having kinetic energies as low as 3.5 eV were used.

The existence of peaks in the plots of SSB yield versus electron kinetic energy, combined with earlier knowledge from the Burrow group of the energies<sup>4</sup> at which DNA's four bases'  $\pi^*$  orbitals attach electrons, led the authors of ref 2 to suggest that the SSBs likely occur by formation of a metastable resonance anion state. That is, the incident electron was postulated to be captured to form an anion that likely involves occupancy of a base  $\pi^*$  orbital, after which some bond (n.b., in ref 2 it is not determined which bond breaks) is ruptured to cause the SSB. However, because the SSB peaks occurred at energies ( $>3.5 \text{ eV}$ ) considerably above the lowest base  $\pi^*$  anion-state energies of the bases, the authors of ref 2 suggested that so-called core-excited resonances are likely involved. These resonances involve, for example, attaching an electron to a  $\pi^*$  orbital and simultaneously exciting another electron from a  $\pi$  to a  $\pi^*$  orbital. It is the combination of the energy associated with the endothermic attachment of the electron to a  $\pi^*$  orbital and that needed to effect the  $\pi \rightarrow \pi^*$  excitation that is provided by the kinetic energy of the free electron.

## II. Review of Our Earlier Studies

It thus appeared that electrons with energies  $>3.5 \text{ eV}$  could attach to DNA bases and induce SSBs. However, which bonds are broken in the SSBs and the details of the mechanism of bond rupture were not yet resolved. We therefore undertook three theoretical studies<sup>5–7</sup> in which we excised<sup>8</sup> a base-sugar–phosphate unit (an example is shown in Figure 1) of DNA and used theoretical simulations to further probe these matters.

The model systems treated in refs 5–7 consisted of a cytosine- or thymine- containing fragment (shown in Figure 1) but with the negative charge in each phosphate group terminated by protonation, which we used to simulate the presence of the tightly associated counteractions that certainly are present in the dry samples of ref 2. As a result, the systems we studied have no net charge prior to attaching a single excess electron.

We chose a cytosine- or thymine-containing fragment because these bases have the lowest-energy  $\pi^*$  orbitals, and we decided to consider whether even lower-energy electrons than those studied in ref 2 might also induce SSBs. That is, we did not focus on the core-excited ( $>3.5 \text{ eV}$ ) electron attachment processes thought to be operative in ref 2. We instead proceeded to consider whether even lower-energy electrons could cause SSBs by attaching to DNA's bases. In particular, we considered what happens when an electron is attached to a base  $\pi^*$  orbital but no further excitation of the electronic structure occurs. As such, our studies should be viewed as inspired by the findings of ref 2 but by no means as direct simulations of ref 2's experiments. Rather, our efforts probe SSBs formed by processes related to but distinct from those of ref 2; in the jargon of electron-scattering resonances, we studied shape resonance anions whereas ref 2's data was suggested to relate to so-called core-excited resonances in which an electron is added to a virtual orbital and a second electron is excited from an occupied to a virtual orbital.

\* Corresponding author. E-mail: simons@chemistry.utah.edu.

<sup>†</sup> University of Utah.

<sup>‡</sup> University of Gdansk.

<sup>§</sup> A holder of a Foundation for Polish Science (FNP) Award.

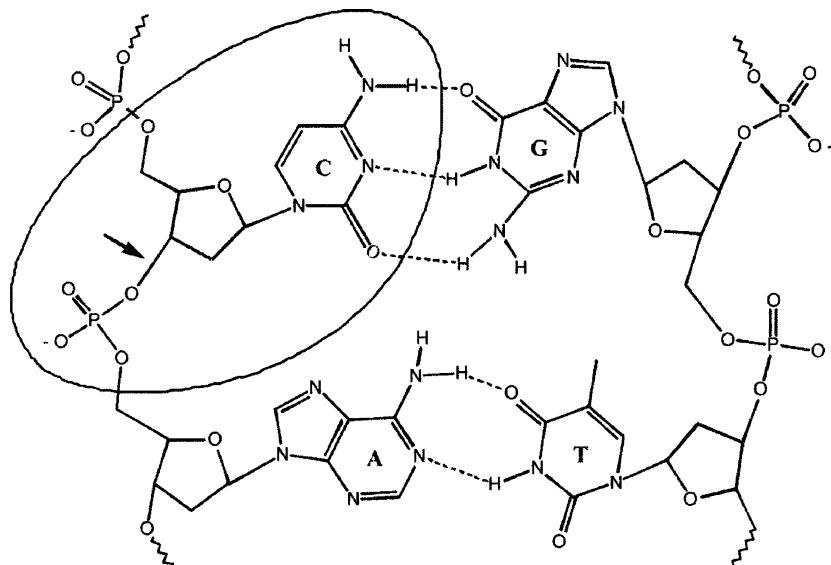


**Figure 1.** Fragment of DNA excised for study in refs 5 and 6 showing the cytosine–sugar–phosphate fragment and the bond that ruptures (in ref 7 the fragment of DNA studied contains thymine instead of cytosine).

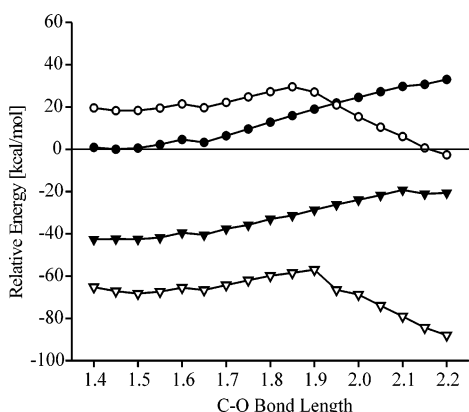


**Figure 2.** Energies of neutral (filled symbols) and anionic (open symbols) cytosine-containing DNA fragment vs C–O bond length (Å) as isolated species (top two plots) and with  $\epsilon = 78$  (bottom two plots) (taken from ref 6).

**TABLE 1: Barriers (kcal mol<sup>-1</sup>) along the C–O Bond Length for Various Electron Kinetic Energies  $E$  (eV) and Various Solvent Dielectric Constants  $\epsilon$  for the Cytosine–Sugar–Phosphate Fragment (from Ref 6)**

| electron energy $E$ (eV)      | 0.2 | 0.3 | 0.8 | 1.0 | 1.3 | 1.5 |
|-------------------------------|-----|-----|-----|-----|-----|-----|
| barrier ( $\epsilon = 1.0$ )  | 16  | 15  | 12  | 11  | 9   | 8   |
| barrier ( $\epsilon = 4.9$ )  | 18  | 18  | 13  | 10  | 10  | 8   |
| barrier ( $\epsilon = 10.4$ ) | 19  | 20  | 14  | 10  | 10  | 8   |
| barrier ( $\epsilon = 78$ )   | 28  | 22  | 11  | 9   | 5   | 5   |

**TABLE 2: Barriers (kcal mol<sup>-1</sup>) along the C–O Bond Length for Various Electron Kinetic Energies  $E$  (eV) and Various Solvent Dielectric Constants  $\epsilon$  for the Thymine–Sugar–Phosphate Fragment (from Ref 7)**

| electron energy $E$ (eV)      | 0.25 | 0.3 | 0.45 | 1.0 |
|-------------------------------|------|-----|------|-----|
| barrier ( $\epsilon = 1.0$ )  | 13   | 13  | 10   | 8   |
| barrier ( $\epsilon = 4.9$ )  | 17   | 15  | 14   | 10  |
| barrier ( $\epsilon = 10.4$ ) | 18   | 17  | 14   | 11  |
| barrier ( $\epsilon = 78$ )   | 25   | 19  | 15   | 7   |

**A. Cytosine or Thymine Electron Attachment.** The primary findings of two of our earlier studies are summarized below in Figure 2, Table 1, and Table 2. In Figure 2, we plot the energy of the cytosine–sugar–phosphate fragment as the phosphate–sugar O–C bond is stretched<sup>9</sup> both in the absence of the attached electron and with an electron attached to cytosine’s lowest  $\pi^*$

orbital. We plot these data both for an isolated (i.e., nonsolvated) fragment as is representative of the samples in ref 2 and when solvated by a medium characterized by a dielectric constant  $\epsilon$  of 78. We performed the solvated-fragment simulations to gain some idea of how large an effect solvation might have on the SSB formation process we were considering.

The two crucial observations to make in Figure 2 are

(1) that the anion surface has a barrier near 1.9 Å and subsequently drops to lower energy as  $R$  is further increased, while the neutral-fragment surface monotonically increases with  $R$  indicative of homolytic cleavage of the C–O bond and

(2) that the anion is electronically metastable with respect to electron autodetachment when solvation is absent but can be rendered electronically stable if solvation is sufficient.

As we explain below, the barrier on the anion surface and its physical origin play central roles in the mechanism and rates of SSB formation that we introduced in ref 6. Moreover, the stability or metastability of the  $\pi^*$  anion determines whether SSB formation does or does not have to compete with electron autodetachment and thus plays a crucial role in determining the final yield of SSBs.

Our data on the cytosine-containing DNA fragment (Table 1) are qualitatively the same as those we obtained for a thymine-containing species (Table 2), although there are quantitative differences in the bond-cleavage rates and how these rates depend on electron energy  $E$  and solvation strength  $\epsilon$ .

In our earlier studies, we carried out simulations for a range of energies  $E$  for the electron that attaches to the  $\pi^*$  orbital because these metastable  $\pi^*$  anion states have substantial Heisenberg widths that derive from their short lifetimes.<sup>4</sup> We varied the electron energy  $E$  to span the reasonable range of these widths. For each  $E$  value, we carried out simulations with the cytosine (or thymine)–sugar–phosphate unit surrounded by a dielectric medium of various solvation strengths (as characterized by the dielectric constant  $\epsilon$  in the polarized continuum model (PCM) of solvation).<sup>10</sup> In Tables 1 and 2, we summarize how the barrier on the anion surface depends on the electron kinetic energy  $E$  and the solvent dielectric strength  $\epsilon$ .

The yield for SSB formation per electron that strikes a DNA sample depends on several factors only one of which we have addressed:

(1) The probability for attachment of the electron to the  $\pi^*$  orbital of the base and its electron energy dependence.

(2) The Franck–Condon factors that arise in the capture cross-section. Because there are small geometry changes accompanying adding an electron to a base  $\pi^*$  orbital, these factors are expected to be large and favorable for the cases under study.

(3) The probability that, once the electron has been captured into a  $\pi^*$  orbital, a bond cleavage occurs.

In the present study, as in our past efforts, we focus only on the third factor. As stated above, we believe the Franck–Condon contributions will not attenuate the rates appreciably. Moreover, we know from ref 2 that the yield of SSBs is in the range of  $10^{-4}$  per incident electron, and so the attachment probability cannot be smaller than  $10^{-4}$ , and its  $E$ -dependence is known from the measurements of ref 4 where electron attachment to DNA bases was studied. So, the focus of our work remains on determining what happens after an electron is attached to a DNA base.

From the above barrier data, we are able to estimate the rates of C–O bond breakage after electron attachment by taking the frequency at which a typical C–O bond vibrates (ca.  $10^{13} \text{ s}^{-1}$ ) and multiplying by the probability  $P$  that thermal motions can access the barrier height  $\Delta$ :  $P = \exp(-\Delta/kT)$ . We found these barriers  $\Delta$  to vary from ca. 5 to 28 kcal/mol and from 7 to 25 kcal/mol for cytosine- (Table 1) and thymine-containing (Table 2) fragments, respectively; they are smallest at higher  $E$ -values and they depend on the solvation environment as shown in Tables 1 and 2.

It was thus suggested in refs 5–7 that accessing the barrier on the  $\pi^*$  anion surface would be the rate-limiting step in SSB formation (after electron capture) by the  $\pi^*$  base anion mechanism that we suggested. Also, barrier heights of 5, 10, 15, 20, and 25 kcal mol $^{-1}$  are predicted (using rate =  $10^{13} \exp(-\Delta/RT) \text{ s}^{-1}$  and a temperature of 298 K as in ref 2) to produce C–O rupture rates of  $6.3 \times 10^9$ ,  $1.3 \times 10^6$ ,  $2.7 \times 10^2$ ,  $6 \times 10^{-2}$ , and  $1 \times 10^{-5} \text{ s}^{-1}$ . For example, when a 1 eV electron attaches to cytosine, the barrier height is 11 kcal mol $^{-1}$ , and we predict phosphate–sugar O–C  $\sigma$  bond cleavage occurs at  $10^6 \text{ s}^{-1}$ .

So, what did we suggest is involved in the electron-induced SSB formation process? First, it is important to recall that the unsolvated anion (as in ref 2) can undergo autodetachment (at a rate of ca.  $10^{14} \text{ s}^{-1}$ ). Also, it is believed that the attached electron can hop to a neighboring  $\pi$ -stacked base (at a rate of ca.  $10^{12} \text{ s}^{-1}$ ). Therefore, the bond-cleavage rates mentioned above suggest that only 1 in ca.  $10^8$  such  $\pi^*$  anions will subsequently undergo SSB formation; most will autodetach, and electron migration from base to base will be ca.  $10^4$  times faster than that of bond cleavage. However, our data also suggest that the base anion can be rendered electronically stable<sup>11</sup> even when modestly solvated (e.g., as in vivo), in which case competition with autodetachment is no longer an issue; now, base-to-base electron hopping would be the primary competitor for bond cleavage, so the yield of SSB formation would be much greater than in the rather dry samples of ref 2.

**B. Phosphate Group Attachment.** In addition to identifying the barriers to C–O bond rupture for cytosine and thymine fragments, we also considered the fate of electrons that might attach directly to a (neutralized) phosphate fragment. Other workers had proposed, on the basis of theoretical results,<sup>12</sup> that rather than attaching to DNA base  $\pi^*$  orbital as we had originally suggested,<sup>5–7</sup> it may be possible for a very low energy electron to attach directly to the phosphate moiety to form a  $\text{P}\cdot\text{--}\text{O}^-$  radical anion which might live long enough to subse-

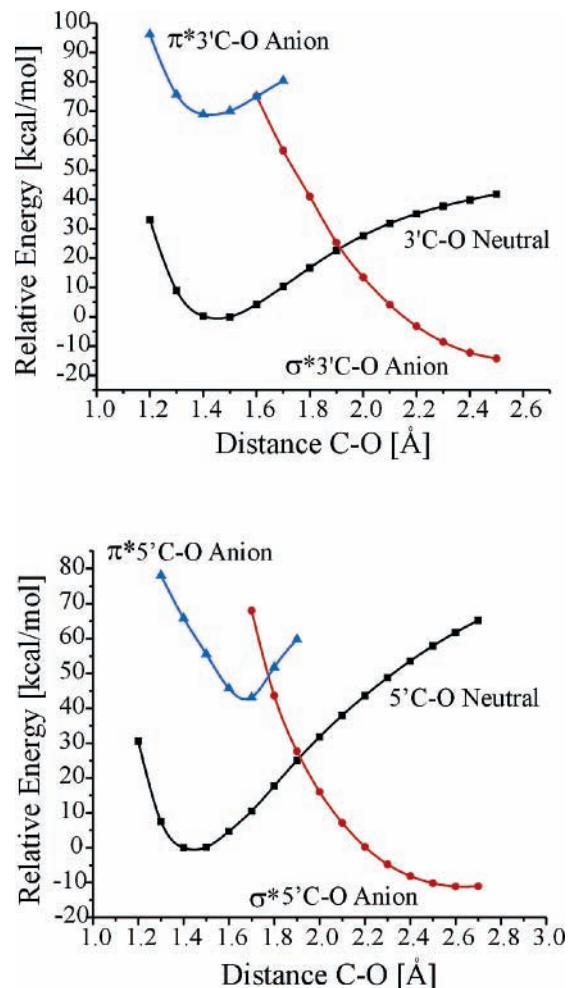


**Figure 3.** Energies of neutral,  $\pi^*$  anion, and  $\sigma^*$  anion for 3'C–O (top) and 5'C–O (bottom) bond rupture vs C–O bond length.

quently induce rupture of a 3' or 5' P–O  $\sigma$  bond. Even though the theoretical approach in ref 12 is valid at geometries where the anion is electronically stable, it is not appropriate for those geometries at which the  $\pi^*$  and the  $\sigma^*$  states are not electronically stable. Specifically, the anion energies shown in Figure 2 of ref 12 have, at geometries where the anion is metastable, undergone variational collapse and thus represent nothing more than the energy of the neutral molecule plus a free electron. As a result, the conclusions reached in ref 12 concerning the metastable states are not valid. Therefore, we decided to improve the description of ref 12 by employing the so-called stabilization method<sup>13,14</sup> to obtain the resonance-state energies for the  $\pi^*$  state and the  $\sigma^*$  state in the region where these states are not stable.<sup>15</sup> In Figure 3, we show the neutral and  $\pi^*$  and  $\sigma^*$  diabatic anion curves obtained using the stabilization method for fragmentation of the 3' C–O and 5' C–O bonds, respectively.

Our findings led us to conclude the following:

(1) Unlike what was suggested in ref 12, electrons having kinetic energies near 0 eV cannot attach directly at significant rates (we estimated the rates to be  $10^5 \text{ s}^{-1}$ ) to DNA's phosphate units (even if these units are rendered neutral by counterions).

(2) Electrons with energies in the 2–3 eV range (see Figure 3) can attach directly (vertically) to DNA's (neutralized) phosphate group's P=O  $\pi^*$  orbital and form a metastable  $\pi^*$  anion which, by coupling to the repulsive O–C  $\sigma^*$  anion state, can lead to C–O bond cleavage. Thus, such anions can induce phosphate–sugar O–C  $\sigma$  bond cleavages but only at rates that

we estimated to be ca.  $10^6 \text{ s}^{-1}$  with the rates determined largely by the heights of the barrier on the adiabatic  $\pi^*/\sigma^*$  anion surface.

In the present work, we are extending these earlier studies to now examine the effects of  $\pi$ -stacking by using three cytosine–sugar–phosphate units as our model compound. We also consider the possibility of the low-energy electrons breaking the base–sugar N–C bond rather than the sugar–phosphate C–O bond. As we demonstrate here,  $\pi$ -stacking has significant effects on the rates of SSB formation via this mechanism.

### III. Methods

**A. The Fragment Studied.** To examine the entire DNA molecule using the type of ab initio electronic structure tools needed for this study is currently computationally prohibitive. Therefore, we had to select a portion of the full DNA<sup>16</sup> molecule that would be representative both of the electron attachment and the bond rupture events that we wish to examine. In this study, we choose to excise a short fragment of a single DNA strand that consists of three nucleotides, each of which is built of the following:

(1) a cytosine base that contains the delocalized  $\pi$ -orbital system to whose lowest  $\pi^*$  orbital an electron could be attached to and

(2) a sugar moiety characteristic of all such fragments of DNA, which connects the cytosine to

(3) a neutralized phosphate group attached to the sugar by the C–O bond that is ruptured in most of the SSBs we consider here. In Figure 4, the fragment that we excised from DNA to study in this research effort is shown, and the C–O bond broken in the SSBs is labeled with an arrow.

Therefore, the whole system studied here mimics a CCC codon such as that responsible for coding proline in biological cells.

**B. Ab Initio Strategy.** Having chosen the representative fragment, our strategy was to proceed as follows:

(1) We “terminated” the  $-\text{OPO}_3^{-1}$  radical centers (formed when we cut bonds within the DNA) of our fragment by adding H atoms; we also protonated the  $-\text{OPO}_3^{-1}$  anion sites to neutralize them.<sup>5–7</sup> The former was done to eliminate the radical centers generated by our artificial excising of the fragment from intact DNA. Such centers, if not so terminated, would provide artificial electron attachment sites that would obscure the  $\pi^*$  binding site we wish to emphasize. The protonation was used to render the sample neutral as likely is the case in the experiments of ref 2.

(2) We applied a two-layered ONIOM<sup>17–19</sup> method to carry out a series of ab initio electronic structure calculations on the neutral and anion formed by adding an electron to the  $\pi^*$  LUMO of the central cytosine unit. The model system (described at the “high” layer in ONIOM theory) is the central nucleotide and it is treated with the SCF method and 6-311+G\* basis sets,<sup>20</sup> whereas for the two terminal nucleotides (“low” layer), we used 4-31G basis sets. In Figure 4, the “higher” layer is represented by balls and sticks while tubes are used to indicate the “lower” layer. We could not utilize a molecular mechanics description of the “low” layer because we wanted to study the effects of the  $\pi$  orbitals of this layer on the energy of the  $\pi^*$  anion formed by placing an electron into a  $\pi$  orbital of the neighboring “high” layer.

(a) For the neutral model, the sugar–phosphate C–O bond length  $R$  of the central nucleotide was stretched, in steps of 0.05 Å, from 1.40 Å, which is near its equilibrium length, to large

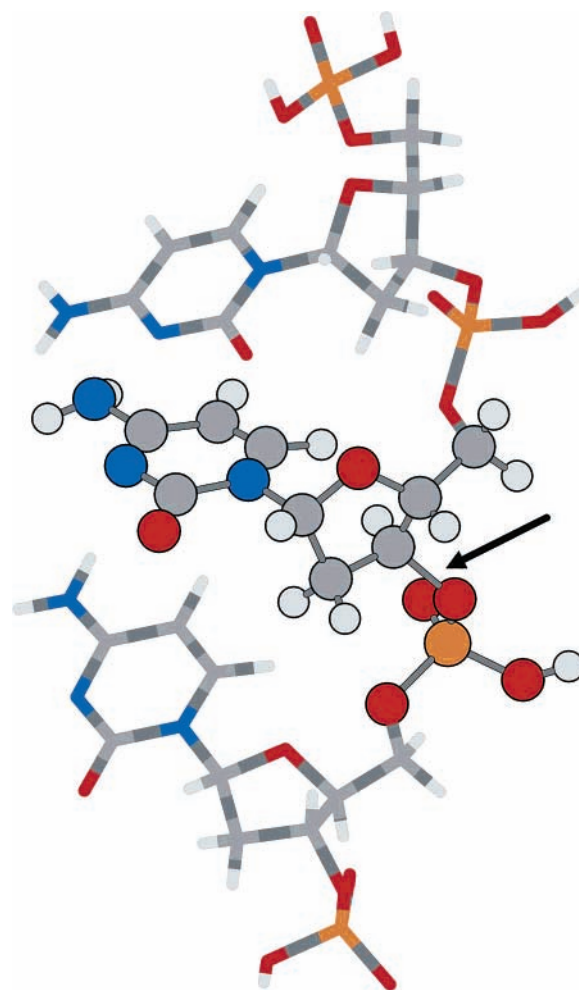


**Figure 4.** Fragment of DNA showing the three nucleotides containing cytosine–sugar–phosphate units. The C–O bond cleaved in SSB formation is marked with an arrow.

distances (2.20 Å) where the C–O bond is largely broken and the SSB has begun.

(b) At each value of  $R$ , the other internal coordinates of the central nucleotide (corresponding to the “higher” layer) of the neutral DNA fragment were varied to minimize the electronic energy (computed at the restricted self-consistent field (RHF) level for this closed-shell species). To preserve the  $\pi$ -stacking of the whole system, the two terminal nucleotides were kept geometrically frozen during this optimization.

(3) For the  $\pi^*$  anion, we repeated steps a and b above but used the unrestricted Hartree–Fock (UHF) approximation for this open-shell system in which the excess electron resides in the central cytosine’s  $\pi^*$  orbital.

This is the same kind of strategy used in our earlier studies except for our use of the ONIOM method to handle the three-nucleotide system examined here.

**C. Treating Metastable States.** Because the  $\pi^*$ -anion is not an electronically stable species but is metastable with respect to electron loss, we had to take additional measures to make sure that the energy of the adiabatic state of the anion relative to that of the neutral fragment shown in Figure 5 was correct. In particular, we know from ref 4 and from our own earlier work at what energy range (n.b., these metastable states have significant Heisenberg widths) the low-lying  $\pi^*$  anion states occur. To describe attaching an excess electron of a given energy  $E$  to the lowest  $\pi^*$ -orbital of the central cytosine with an energy within a given range, we needed to alter our atomic orbital basis

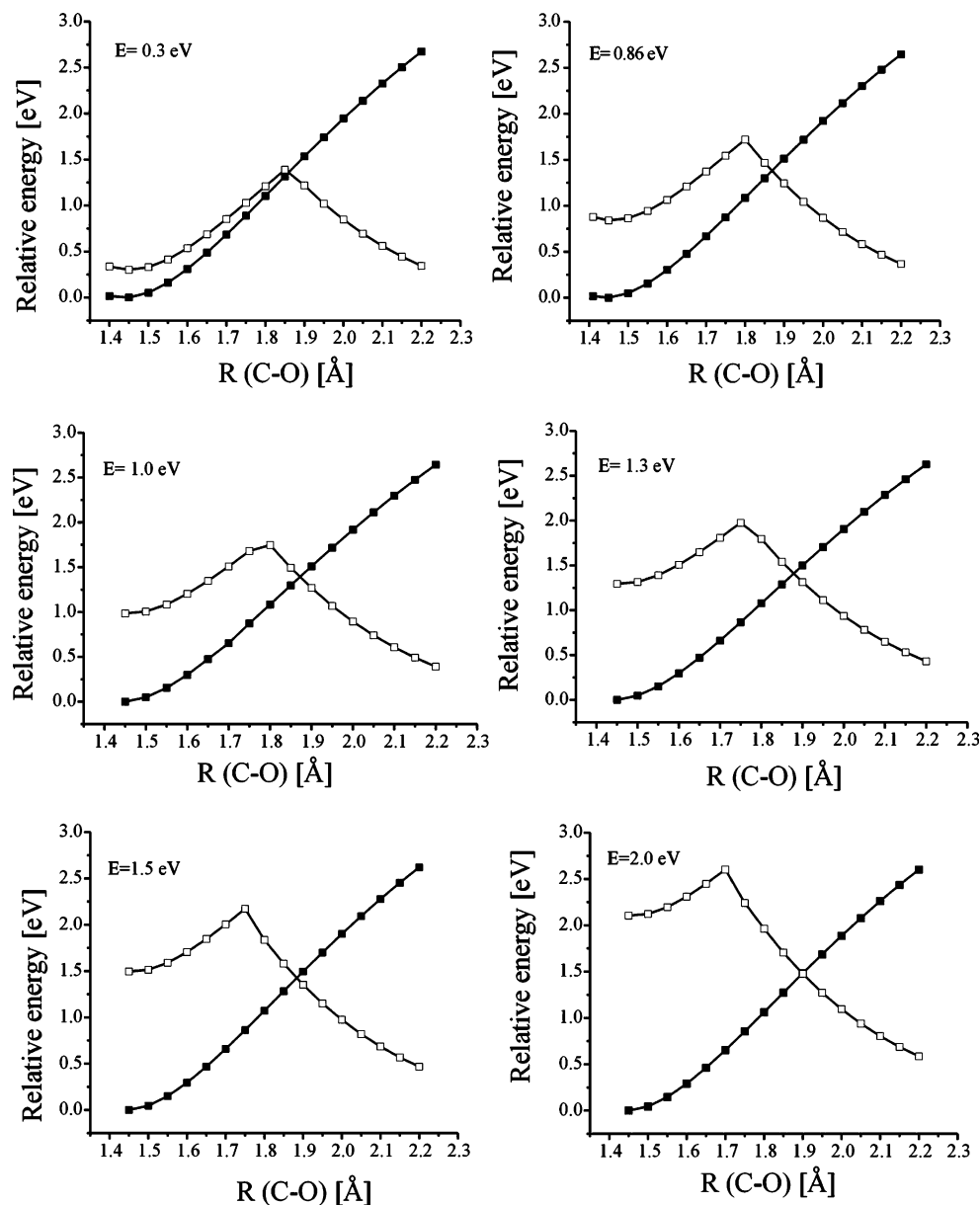


**Figure 5.** Energies of neutral fragment (solid square symbols) and of the  $\pi^*$ -anion (open square symbols) fragment at various electron energies  $E$ .

set to produce a  $\pi^*$ -orbital having such an energy. We did so by scaling the exponents of the most diffuse  $\pi$ -type basis functions on the atoms within the central cytosine ring to generate a lowest  $\pi^*$ -orbital whose UHF anion would have the specified energy (relative to the neutral). Of course, we had to perform independent orbital exponent scaling to achieve  $\pi^*$ -state energies of 0.3, 0.86, 1.0, 1.3, 1.5, and 2.0 eV. By scaling the exponents of the atomic orbital basis functions, we are thus able to model attaching an electron with the desired kinetic energy.

Since the inclusion of solvent effects is not possible while performing ONIOM calculations, we had to limit our approach to the isolated CCC oligomer. However, as described in the Introduction, solvent effects and their influence on the SSB rates were discussed in our preceding papers and are not expected to produce substantially different results in the present model system except for rendering electron autodetachment no longer a competitive pathway when operative.

The energy profiles that we obtain as functions of the C–O bond length labeled in Figure 5 describe variation in the

electronic energy of the cytosine-containing fragment (central nucleotide) and its anion with all other geometric degrees of freedom of the central fragment “relaxed” to minimize the energy. In duplex DNA, there clearly are constraints placed on the geometry of the cytosine–dextyribose–phosphate groups (e.g., hydrogen bonding and  $\pi$ -stacking) that do not allow all geometric parameters to freely vary. As such, the energy profiles we obtain likely provide lower bounds to the barriers that must be overcome to effect C–O bond cleavage. However, we found that the changes in bond lengths ( $<0.04$  Å) and valence angles ( $<5^\circ$ ) are quite small as we “stretch” the C–O bond. Hence, we do not think the unconstrained energy profiles result in qualitatively incorrect barriers.

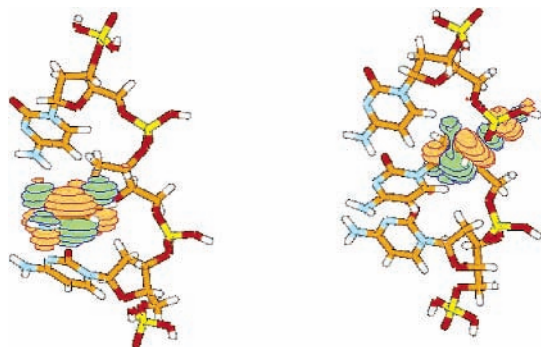
All calculations were performed using the Gaussian 03<sup>21</sup> suite of programs, and the three-dimensional plots of the molecular orbitals were generated with the MOLDEN program.<sup>22</sup>

#### IV. Results

**a. Energy Profiles.** In Figure 5, we show plots of the electronic energies of the neutral and  $\pi^*$ -anion species for the

**TABLE 3: Barriers (kcal/mol) and C–O Bond Lengths  $R$  (Å) at the Barrier for Various Electron Energies  $E$  (eV) (for the Three-Nucleotide System)**

| electron energy $E$ | 0.3  | 0.86 | 1.0  | 1.3  | 1.5  | 2.0  |
|---------------------|------|------|------|------|------|------|
| barrier (gas phase) | 25   | 20   | 18   | 16   | 15   | 11   |
| $R$ at barrier      | 1.85 | 1.80 | 1.80 | 1.75 | 1.75 | 1.70 |

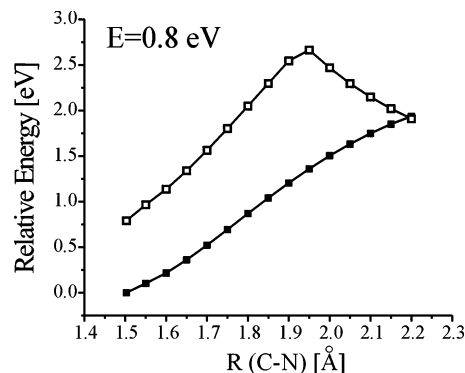
**Figure 6.** Orbital occupied by the attached electron on the central cytosine (left) and for the elongated C–O bond lengths (right) where the electron has migrated toward the phosphate group.

energy  $E$  of the attached electron ranging from 0.3 to 2.0 eV. The  $\pi^*$ -anion energy profiles suggest that C–O bond rupture requires surmounting an 11–25 kcal/mol barrier (depending on the electron energy  $E$ ) but that the fragmentation process is exothermic in all cases. As we noted in our earlier work, the exothermicity results primarily from the large electron affinity ( $>4$  eV) of the neutralized phosphate group generated when the C–O bond ruptures. In Table 3, we collect from Figure 5 values of the barrier heights along the C–O bond length for various  $E$  values, and we show the value of  $R$  at which the barrier occurs in each case. As we found in our earlier cytosine and thymine studies,<sup>6,7</sup> the barrier occurs at nearly the same  $R$  value for all  $E$  values, although there seems to be a trend to smaller  $R$  values at higher  $E$ .

Of course, a primary objective of the present study was to determine how  $\pi$ -stacking alters rates of SSB formation. Therefore, we compare the barrier heights for the single cytosine–sugar–phosphate unit (Table 1) with those obtained for the fragment containing three nucleotides (Table 3), and  $\pi$ -stacking seems to increase the barrier heights by ca. 8 kcal/mol. As a result,  $\pi$ -stacking can be expected to substantially lower the predicted rates of SSB formation compared to our predictions in refs 5–7.

In Figure 6, we show the orbital containing the excess electron at two  $R$ -values. At the smaller  $R$ , the electron is localized on the central cytosine  $\pi^*$ -orbital, but as  $R$  moves beyond ca. 1.9 Å, the electron moves through the virtual orbitals of the adjoining deoxyribose and onto the phosphate unit. In our earlier work,<sup>6</sup> we showed that the rate of electron transfer through the sugar group is fast compared to the rate of accessing the barrier on the anion energy surface, so the barrier-access rate is the rate-limiting step in SSB formation.

**b. Predicted Rates of SSB Formation.** To estimate the rates of SSB formation for the CCC codon, we consider thermal activation of the vibrations of the C–O bond that must rupture. As is typical of most C–O single bonds, this bond is expected to vibrate at a rate of ca.  $3 \times 10^{13} \text{ s}^{-1}$ . The probability  $P$  that this C–O bond stretches, through thermal activation at 298 K, enough to surmount a barrier of  $\Delta$  can be approximated by  $P = \exp(-\Delta(505)/298)$ , where  $\Delta$  is given in kcal/mol and  $505 = 1/R$  with  $R$  being the ideal gas constant  $R = 1.98 \times 10^{-3} \text{ kcal/mol}\cdot\text{K}$ . Hence, an estimate of the average rate of SSB formation

**Figure 7.** Energies of the neutral (solid square symbols) and of the  $\pi^*$ -anion (open square symbols) DNA fragment vs C–N bond length (Å) as isolated species at electron energy  $E = 0.8$  eV.

can be obtained by multiplying the vibrational frequency by the probability of accessing the barrier:  $10^{13} \exp(-\Delta(505)/298) \text{ s}^{-1}$ . Using barrier heights  $\Delta$  of 11, 15, 16, 18, 20, and 25 kcal/mol, which characterize the range shown in Table 3, we obtain SSB rates of  $0.8 \times 10^5$ ,  $2.7 \times 10^2$ ,  $1.9 \times 10^1$ ,  $6.4 \times 10^{-1}$ ,  $6 \times 10^{-2}$ , and  $1 \times 10^{-5} \text{ s}^{-1}$ , respectively. Since the autodetachment rate of the  $\pi^*$ -state is ca.  $10^{14} \text{ s}^{-1}$ , and the rate of migration to a neighboring base is ca.  $10^{12} \text{ s}^{-1}$ , the rate of SSB formation is predicted to generate SSBs at rates 9 or more orders of magnitude below that of detachment. Thus, it seems unlikely that SSBs can be induced at significant rates in CCC codon by electron attachment to the cytosine base's  $\pi^*$  orbital for energies ranging from 0.3 to 2.0 eV when solvation does not render autodetachment inoperative. However, our previous findings suggest<sup>5–7</sup> that even modest solvation can make the anion electronically stable. Thus, solvation effects seem to be crucial for allowing the  $\pi^*$  state to produce SSBs in any significant yield.

### c. Examination of Sugar–Cytosine C–N Bond Cleavage.

In addition to the present study on effects of base  $\pi$ -stacking on damage to DNA by low-energy electrons, we also examined the possibility of breaking a sugar–cytosine C–N bond. As our earlier studies made clear, it is the electronic stability of the anion formed when bond cleavage occurs that provides the thermodynamic driving force (and thus the low barriers on the anion surfaces) for bond breaking. We thought that the anion formed when a sugar–cytosine C–N bond breaks may be stable enough to make this bond cleavage also facile, so we decided to address this issue.

In Figure 7, we plot the energy of the cytosine–sugar–phosphate fragment as the sugar–cytosine C–N bond is stretched both for the neutral and  $\pi^*$ -anion species for the energy  $E = 0.8$  eV of the attached electron (this energy was in the range of the cytosine  $\pi^*$  orbital energy as discussed earlier).

The neutral's curve shows that, as expected, it is energetically quite endothermic to rupture the C–N bond. Thus, it is unlikely that SSBs can occur at 298 K (where the experiments of ref 2 took place) or even at significantly elevated temperature if the fragment remains neutral (i.e., does not attach an electron). The  $\pi^*$ -anion energy profile suggests that C–N bond rupture requires surmounting a 43 kcal/mol barrier. Recall that the barrier height calculated for the same energy of the attached electron ( $E = 0.8$  eV) for C–O bond cleavage in cytosine–sugar–phosphate is 12 kcal/mol. Thus, we conclude that it is unlikely that SSBs can occur at any significant rate via sugar–cytosine C–N bond rupture. Of course, in living organisms, other damage mechanisms (e.g., oxidative damage, protonation, etc.) are also operative and such C–N bonds may be involved

in those events; our conclusions only apply to the electron-induced bond breakage studied here.

## V. Summary

We studied the effects of base  $\pi$ -stacking on the predicted rates of SSB formation in DNA caused by low-energy electrons. In addition, we also studied the possibility of breaking the base–sugar N–C bond by such low-energy electrons. On the basis of our ab initio calculations we suggest that

(1) An electron having kinetic energy  $E$  in the range 0.3–2.0 eV (as studied here) can attach to the lowest  $\pi^*$ -orbital of cytosine. This state has a maximum in its attachment cross-section near 0.5 eV but the cross section extends considerably above and below this energy; this is why we compute rates for  $E$  values between 0.3 and 2.0 eV. The incident electron cannot enter the C–O  $\sigma^*$ -orbital directly because this orbital's energy is too high when the C–O bond is near its equilibrium distance.

(2) As the  $\pi^*$  anion's C–O bond vibrates (with frequency  $\nu$ ) under thermal excitation, it has some (albeit low) probability of reaching a critical distortion at which the C–O bond's  $\sigma^*$ -state and the base's  $\pi^*$ -state become nearly degenerate. The energy  $\Delta$  required to access such a stretched C–O bond plays a crucial role in determining the rate (given as  $\nu \exp(-\Delta/RT)$ ) of C–O bond cleavage and thus of SSB formation. We find these barriers  $\Delta$  to vary from ca. 11 to 25 kcal/mol in the CCC codon.

(3) The inclusion of  $\pi$ -stacking effects causes an increase of the energy barriers  $\Delta$  and thus a corresponding decrease of rates of SSB formation to an extent that renders SSB formation rates in the CCC codon to lie below  $0.8 \times 10^5 \text{ s}^{-1}$  for  $E \leq 2.0 \text{ eV}$ . Thus, in the absence of solvation (i.e., when the anion state is unstable with respect to autodetachment), SSB formation does not compete substantially with electron loss. However, when solvation renders the anion stable, SSB formation can occur at the computed rates and with substantial yield.

(4) Since the barrier height for sugar–cytosine N–C bond breaking is 43 kcal/mol, which is much higher than the corresponding value estimated for C–O bond breaking, we conclude that such a route is not operative.

**Acknowledgment.** This work was supported by NSF, Grant Nos. 9982420 and 0240387 to J. S., and by the Polish State Committee for Scientific Research (KBN), Grant No. DS/8371-4-0137-4 to P. S. Significant computer time provided by the Center for High Performance Computing at the University of Utah and by the Academic Computer Center in Gdansk (TASK) is also gratefully acknowledged.

## References and Notes

- (1) The subject was the subject of a recent popular science article: Collins, G. P. News Scan, Fatal Attachments: Extremely low energy electrons can wreck DNA. *Sci. Am.* **2003**, September issue, pp 26–28.
- (2) Boudaiffa, B.; Cloutier, P.; Hunting, D.; Huels, M. A.; Sanche, L. *Science* **2000**, *287* (5458) 1658–1662.
- (3) The DNA samples used in ref 2 were quite dry and contained only their structural water molecules. Moreover, their phosphate groups likely

had counterions closely bound to them because the samples did not possess net positive or negative charges. It is very important to keep in mind that all of the experimental and theoretical data discussed in the present paper relate to such neutral samples in which the phosphate groups do not possess negative charges prior to electron attachment.

- (4) Aflatooni, K.; Gallup, G. A.; Burrow, P. D. *J. Phys. Chem. A* **1998**, *102*, 6205–6207.
- (5) Barrios, R.; Skurski, P.; Simons, J. *J. Phys. Chem. B* **2002**, *106*, 7991.
- (6) Berdys, J.; Anusiewicz, I.; Skurski, P.; Simons, J. *J. Phys. Chem. A* **2004**, *108*, 2999.
- (7) Berdys, J.; Skurski, P.; Simons, J. *J. Phys. Chem. B* **2004**, *108*, 5800.
- (8) We terminated with H atoms the –O radical centers and we rendered neutral (by protonation) the negative charge shown in Figure 1 on the phosphate O atom to simulate the presence of the nearby counterion that no doubt is present in the dry samples of ref 2.
- (9) We focused on this particular bond because it was clear to us that its rupture would be thermodynamically favored because of the large ( $>4 \text{ eV}$ ) electron affinity of the phosphate unit that is formed upon its cleavage.
- (10) Miertus, S.; Tomasi, J. *Chem. Phys.* **1982**, *65*, 239–242. Cossi, M.; Barone, V.; Cammi, R.; Tomasi, J. *Chem. Phys. Lett.* **1996**, *255*, 327–335.
- (11) To form such a stable  $\pi^*$  anion, the incident electron would have to enter the base  $\pi^*$  orbital and there would have to be some mechanism (e.g., radiationless relaxation or dissipation of energy to the solvent) to remove the excess energy.
- (12) Li, X.; Sevilla, M. D.; Sanche, L. *J. Am. Chem. Soc.* **2003**, *125*, 13668–13666.
- (13) Hazi, A. U.; Taylor, H. S. *Phys. Rev. A* **1970**, *1109*–1116.
- (14) Simons, J. In *Resonances in Electron–Molecule Scattering, van der Waals Complexes and Reactive Chemical Dynamics*; ACS Symposium Series 263; Truhlar, D. G., Ed.; American Chemical Society: Washington, DC, 1984; pp 3–16.
- (15) Berdys, J.; Anusiewicz, I.; Skurski, P.; Simons, J. *J. Am. Chem. Soc.* **2004**, *126*, 6441–6447.
- (16) The structural parameters of the DNA used in this work were taken from The Protein Data Bank. Berman, H. M.; Westbrook, J.; Feng, Z.; Gilliland, G.; Bhat, T. N.; Weissig, H.; Shindyalov, I. N.; Bourne, P. E. *Nucleic Acids Res.* **2000**, *28*, 235–242.
- (17) Svensson, M.; Humbel, S.; Froese, R. D. J.; Matsubara, T.; Sieber, S.; Morokuma, K. *J. Phys. Chem.* **1996**, *100*, 19357.
- (18) Humbel, S.; Sieber, S.; Morokuma, K. *J. Chem. Phys.* **1996**, *105*, 1959.
- (19) Froese, R. D. J.; Morokuma, K. Hybrid Method. In *Encyclopedia of Computational Chemistry*; Schleyer, P. v. R., Ed.; Wiley: New York, 1998.
- (20) Ditchfield, J. R.; Hehre, W. J.; Pople, J. A. *J. Chem. Phys.* **1971**, *54*, 724. Hehre, W. J.; Ditchfield, R.; Pople, J. A. *J. Chem. Phys.* **1972**, *56*, 2257.
- (21) Frisch, M. J.; Trucks, G. W.; Schlegel, H. B.; Scuseria, G. E.; Robb, M. A.; Cheeseman, J. R.; Montgomery, J. A., Jr.; Vreven, T.; Kudin, K. N.; Burant, J. C.; Millam, J. M.; Iyengar, S. S.; Tomasi, J.; Barone, V.; Mennucci, B.; Cossi, M.; Scalmani, G.; Rega, N.; Petersson, G. A.; Nakatsuji, H.; Hada, M.; Ehara, M.; Toyota, K.; Fukuda, R.; Hasegawa, J.; Ishida, M.; Nakajima, T.; Honda, Y.; Kitao, O.; Nakai, H.; Klene, M.; Li, X.; Knox, J. E.; Hratchian, H. P.; Cross, J. B.; Adamo, C.; Jaramillo, J.; Gomperts, R.; Stratmann, R. E.; Yazyev, O.; Austin, A. J.; Cammi, R.; Pomelli, C.; Ochterski, J. W.; Ayala, P. Y.; Morokuma, K.; Voth, G. A.; Salvador, P.; Dannenberg, J. J.; Zakrzewski, V. G.; Dapprich, S.; Daniels, A. D.; Strain, M. C.; Farkas, O.; Malick, D. K.; Rabuck, A. D.; Raghavachari, K.; Foresman, J. B.; Ortiz, J. V.; Cui, Q.; Baboul, A. G.; Clifford, S.; Cioslowski, J.; Stefanov, B. B.; Liu, G.; Liashenko, A.; Piskorz, P.; Komaromi, I.; Martin, R. L.; Fox, D. J.; Keith, T.; Al-Laham, M. A.; Peng, C. Y.; Nanayakkara, A.; Challacombe, M.; Gill, P. M. W.; Johnson, B.; Chen, W.; Wong, M. W.; Gonzalez, C.; Pople, J. A. *Gaussian 03*, revision A.1; Gaussian, Inc.: Pittsburgh, PA, 2003.
- (22) Schaftenaar, G.; Noordik, J. H. MOLDEN: a pre- and postprocessing program for molecular and electronic structures. *J. Comput.-Aided Mol. Des.* **2000**, *14*, 123.